Study of powder dispersion at the injector exit and its influence on particles thermal and dynamic history

Fadhel Ben Ettouil, Bernard Pateyron, Hélène Ageorges, Mohammed El Ganaoui, Pierre Fauchais

Study of powder dispersion at the injector exit and its influence on particles thermal and dynamic history

F. Ben Ettouil, B. Pateyron, Hélène Ageorges, M. El Ganaoui, P. Fauchais

University of Limoges, SPCT, Limoges, France

Abstract: In plasma spraying, the particles dispersion at the injector exit controls their dynamical and thermal histories (trajectories, velocities, temperatures, melting and vaporization …) which are key parameters for the splat formation at impact and the coating construction. In this paper a model of particles conveyed within the injector is presented and their dispersions in size, velocity and direction are characterized

Keywords: powder feeder, injector, collisions, dispersion angle, velocity distribution

Nomenclature:

A : constant (-)
C : constant (-)
C_D : drag coefficient (-)
D : internal diameter of the injector (m)
d_p : particle diameter (m)
f : friction coefficient (-)
k : Karman constant (-)
k_4 : constant (-)
m_p : particle mass (kg)
r : radius (m)
R : injector radius (m)
Re : Reynolds number (-)
u : velocity (m/s)
u_* : shear velocity (m/s)
u^+ : dimensionless velocity $u^+ = u/u_*$ (-)
U : similarity number of the wall effect (-)
y = R-r distance from the wall (m)
Y : similarity number combining inner and outer variables
y^+ : inner variable $y^+ = y.u^*/\upsilon$ (-)

Greek
δ : dispersion angle (rad)
Φ: azimuthal dispersion angle (rad)
ρ : mass density (kg.m^{-3})
μ : molecular viscosity (Pa.s)
μ_{eff} : suspension viscosity (Pa.s)
ε_s : solid fraction (-)
υ : kinematic viscosity (m^2/s)
τω : wall shear stress (N/m2)
ξ : outer variable $\xi = y/R$ (-)

Indices :
g : gas
p : particle

1. Introduction

At the injector exit, a particle is characterized by four parameters:

- velocity vector amplitude
- velocity vector angle δ within a cone which total angle is generally below 20° (see figure 1)
- velocity vector angle in the direction defined by the angle Φ varying from 0 to 360°
- mass distribution

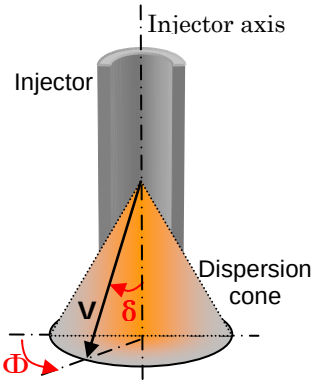

Fig. 1 Cone of particles dispersion at the injector exit

For the same amplitude, the velocity vector angle plays a non negligible role as illustrated in figure 2. It presents the evolution of the surface temperature of two zirconia particles, 25 μm in diameter, both injected with the same injection velocity vector amplitude of 40 m/s, but with two different angles (δ_1=0° et δ_2=10°). It can be seen that the modification of only one parameter of the particle injection changes its thermal history. Similar results are obtained for its trajectory and velocity.

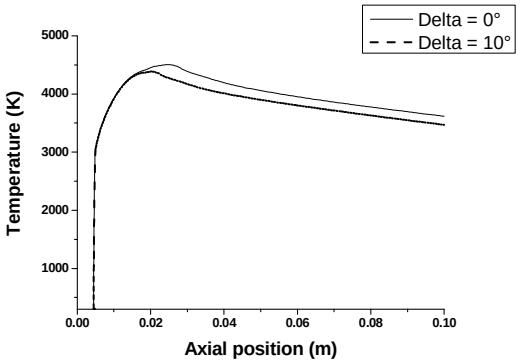

Fig.2: Temperature evolution on the surface of zirconia particles of 25 μm in diameter Injected with different δ angles and Φ=0

This work presents a descriptive model of the transport of particles by a carrier gas inside the cylindrical injector. The model taking into account the size distribution of the particles, the particle collisions between themselves and with the injector wall, makes it possible to obtain the velocity and size distribution of particles at the injector exit.

The adapted strategy in this simulation consists in:

- calculating the gas velocity profile,
- simulating of the size distribution,
- calculating of particle displacements and velocities,
- detecting of particle-particle and particle-wall collisions,
- calculating of displacements and velocities after collisions.

2. Modeling

2.1 Calculation of carrier gas velocity profile

To evaluate the viscosity of the suspension gas-powder, the formula of Einstein has been used [1]

$$\mu_{eff} = \mu_g (1 + 2.5\varepsilon_s)$$

The flow mode is determined by the Reynolds number:

$$\mathrm{Re} = \rho_g u_g D / \mu_{eff}$$

In the case of turbulent flow, a self-similarity of mean-flow is considered [2], it is based on modified log-wake law for turbulent flow [3]. The friction coefficient is written as following:

$$f = \frac{0.3164}{\mathrm{Re}_g^{0.25}} \left(1 + \mathrm{Re}/\, 4.3110^5\right)$$

The wall shear stress is given by:

$$\tau_\omega = \frac{f}{8} \rho_g u_g^2$$

The shear velocity is expressed as follows

$$u_* = \sqrt{\tau_\omega / \rho_g}$$

u^+ being the dimensionless velocity which is given by:

$$u^+ = u(r) / u_*$$

The model considered is based on two composed similarity numbers U and Y, where U is the similarity number representing the pure effect of the wall and Y that combining the inner and outer variables.

$$Y = y^+ \exp\left(-\xi^4 / 4\right)$$

$$U = A.arctg\left(\frac{Y}{A}\right) + \frac{A}{3}.arctg^3\left(\frac{Y}{A}\right) + k_4.arctg^4\left(\frac{Y}{A}\right) + \ln\left[1 + \left(\frac{Y}{C}\right)^{\frac{1}{k}}\right]$$

with A=7, C=107, k=0.43 et k4=-0.52

The dimensionless velocity has been written as follows

$$u^+ = U + 2.\sin^2\left(-\xi^4 / 4\right)$$

Finally, the mean velocity at the radial position r is written as the function of the outer variable and the shear velocity:

$$u(r) = u_* \left(U + 2.\sin^2\left(-\xi^4 / 4\right)\right)$$

2.2 Calculation of particle displacement

Particles are supposed to be spherical, they can collide between themselves and with the wall and they are especially subjected to drag force, which permits to write the momentum equation as follows:

$$m_p \frac{dv_p}{dt} = -C_D.\pi.\frac{d_p^2}{4} \rho_g \frac{\left|u_p - u_g\right|\left(u_p - u_g\right)}{2}$$

2.3 particle-particle collision

Particle-particle collisions are supposed to be elastic and treated with the hard sphere model. Particle parameters after collision (position, velocity, acceleration) are calculated from the conservation equations for momentum and energy.

2.4 particle-wall collision

The particle-wall collision was inspired from the collision synchronization in the domain of dynamic simulation and animation. Two approaches are possible:

- Milencovic method [4]: each object is stopped on its first collision, the collision synchronisation and treatment is made at the end of the time step
- Faure and Galizzi method [5]: the rectification of positions and velocities occurs later after the collision.

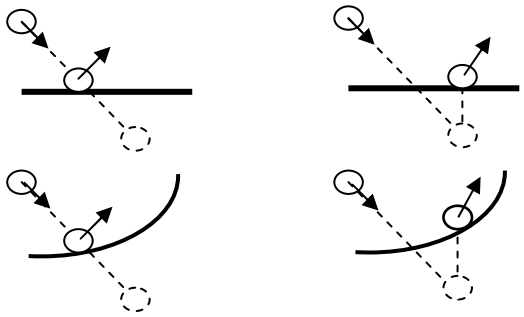

Milenkovic method Faure and Galizzi method

Figure 3: Treatment of particle-wall collision

In this work, the Milencovic method was adopted.

3. Results:

In the following are presented results from the simulation of 5000 zirconia particles (22-45 µm), conveyed within an injector 1.5 mm in diameter. The used carrier gas is argon. The size distribution is presented in figure 4. Gas and powder properties are summarized in table 1.

Table 1: Powder and carrier gas properties

	ρ	Flow rate	Viscosity
Carrier gas: Argon	1,67 kg/m3	4 L/min	2,09 10^{-5} Pa.s
Powder : Zirconia	5800 kg/m3	1 kg/h	-

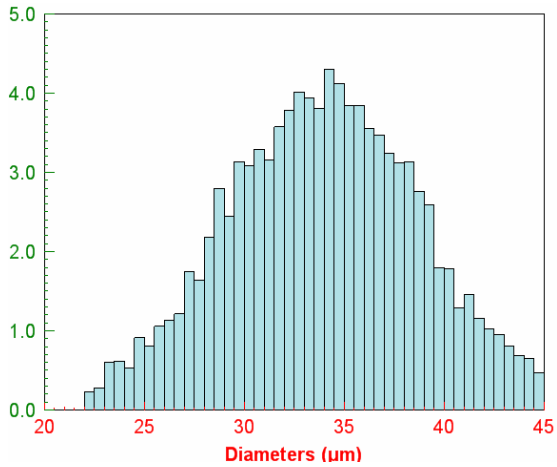

Figure 4: simulated particle size distribution

Figure 5 shows that the spatial distribution of the velocity vectors is uniform in space. According to the surface of a hemisphere the central part corresponds to the smallest surface, thus resulting in an angle distribution close to zero in the injector axis. It is also worth to note that for the initial distribution a maximum angle of 30° was chosen for δ. Of course the initial distribution at the injector inlet should depends on the particle distribution at the connecting pipe outlet and works are in progress to calculate this distribution within the connecting pipe between the powder feeder and the injector.

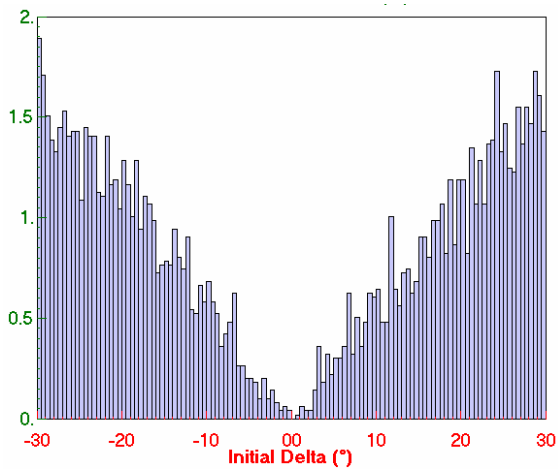

Figure 5: Initial δ angle distribution at the injector inlet

Figure 6 shows that at the injector exit, due to collisions, some particles have a divergence angle higher than 20°, but most of them are within 20° in good agreement with the experimental results. The δ angle distribution evolves along the injector length and after 7 cm, it becomes bimodal and symmetrical. It is clear that it tends after a longer course, to a Gaussian distribution of average zero. The most of δ values are within a cone of 20° and values outside the angle are due to the particle-particle collisions.

Figure 7 shows the δ angle distribution without taking into account particle-particle collision, the dispersion seems to be the previous as the case but with a reduced variation domain.

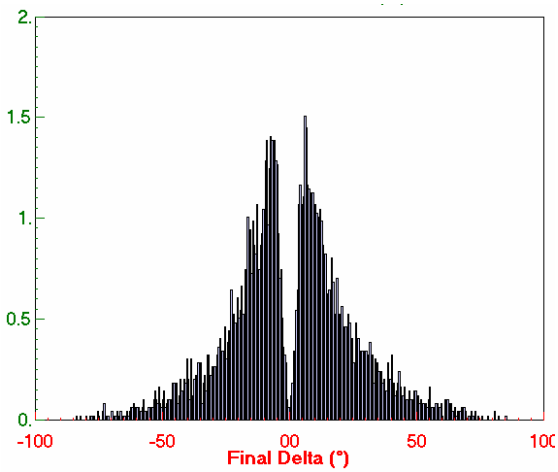

Figure 6: Final δ angle distribution at the 7 cm long injector exit

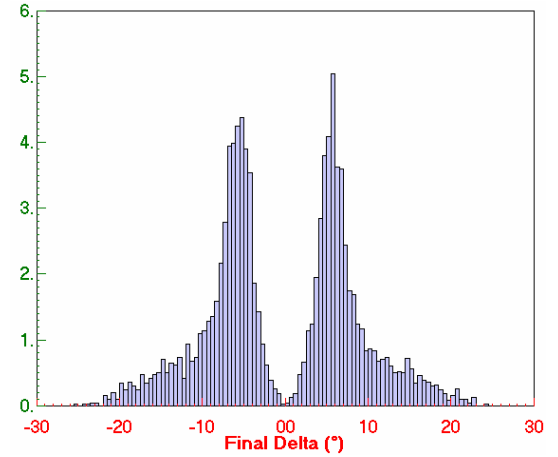

Figure 7: Final δ angle distribution at the injector exit without particle-particle collision

Figure 8 shows the final axial velocity distribution, the initial one being supposed to be randomly uniform. This resulting distribution at the injector exit seems to be Gaussian and is centred on the mean gas velocity

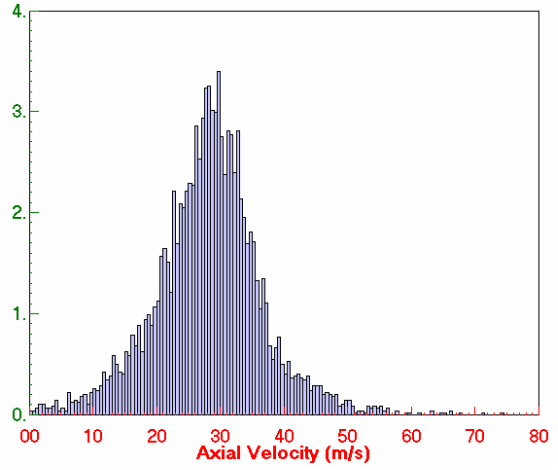

Figure 8: Final axial velocity distribution

Figure 9 illustrates the final δ angle distribution as function of particles size. What ever may be the size class of particles, small or big, the mean value of δ is approximately zero. It seems to confirm that the

dispersion of δ is independent of the particles size.

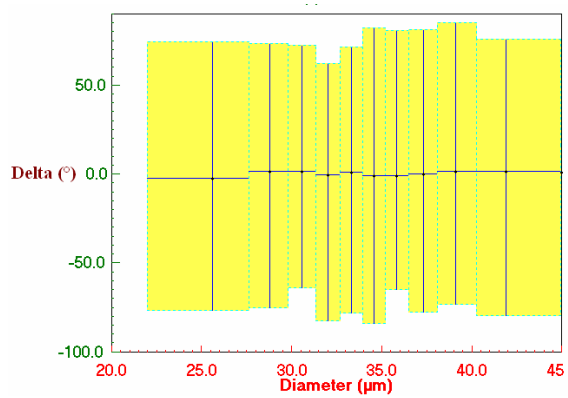

Figure 9: Final δ angle distribution as function of particles size

Figure 10 presents the distribution of the radial velocity as function of the particle size. The geometry of the studied system is symmetric, which explains why this distribution is almost symmetric and centred on zero.

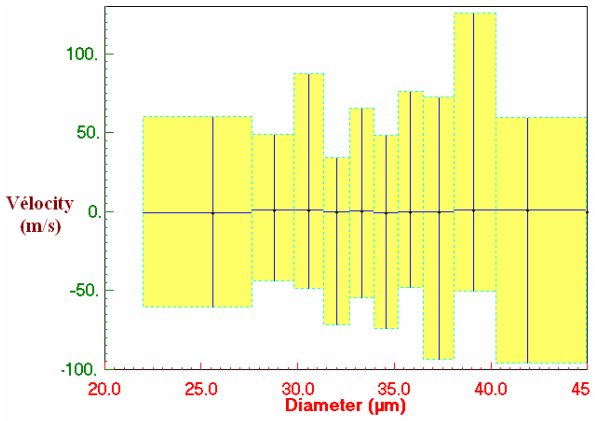

Figure 10: Final radial velocity distribution as function of particles size

4. Conclusions

This paper presents the first results of a model representing the dispersion of particles at the injector exit of a plasma torch. The model developed takes into account the size distribution, the wall-particle and particle-particle collisions. This model is aimed at determining the conditions of particles injection of in a d.c plasma jet according to the working conditions (carrier gas and powder flow rate, injector internal diameter …)

References

[1] T. Kiyoshi, F. Hisamoto, Extension of Einstein's viscosity equation to that for concentrated dispersions of solutes and particles, Journal of Bioscience and Bioengineering, **102,** p 524-528 (2006).

[2] J. Guo. Self-similarity of mean flow in pipe turbulence, AIAA-2006-2885, 36th AIAA Fluid Dynamics Conference, San Francisco, CA, (2006).

[3] Guo, J. and Julien, P. Y. Modified log-wake law for turbulent flow in smooth pipes, Reply to Discussion. J. of Hydraulic Research, IAHR, **43(4)**, p 431-434, (2005)

[4] V. J. Milenkovic, H. Schmidl, Optimization based animation, Computer Graphics Proceedings, Annual conference series: p 37-46, (2001)

[5] O. Galizzi, F. Faure, Animation efficace de solides en contact par modèle physique. Journée Francophones d'Informatique Graphique. AFIG p 167-178, (2002)